Biol. Cybernetics 28, 27—40 (1977)

Biological Cybernetics

Generation of a Locomotory Rhythm by a Neural Network with Recurrent Cyclic Inhibition

W. O. Friesen* and G. S. Stent

Department of Molecular Biology, University of California, Berkeley, California, USA

Abstract. An oscillatory intersegmental neuronal network drives the swimming rhythm of the leech. This network consists of interneurons joined via inhibitory connections to form a series of segmentally iterated, concatenated rings. Recurrent cyclic inhibition in these rings produces a multiphasic activity rhythm. By theoretical analysis of such concatenated interneuronal rings and construction of their electronic analogs it is shown that the interneural network identified in the central nervous system of the leech has properties appropriate for generating the observed motor output.

1. Introduction

Neurophysiological analyses of rhythmic motor routines of both vertebrates and invertebrates have shown that the underlying phasic motor neuron activity pattern is, in many cases, generated by neural elements wholly within the central nervous system (Bullock, 1961). Theoretical considerations inspired by this finding indicate that the primary source of the activity cycle of these elements may be neurons which either are individually capable of undergoing an endogenous polarization rhythm (Alving, 1968), or, if they lack this capacity, are linked synaptically to form an oscillatory network (Wilson, 1966).

The simplest realization of an oscillatory neural network of cells lacking an endogenous polarization rhythm consists of two tonically excited neurons linked reciprocally via inhibitory synapses. The two-cell network must incorporate either an element of fatigue, due to which antecedent activity limits the time during which one neuron can subject its partner to inhibition (Reiss, 1962), or a transient source of excitation, such as that provided by postinhibitory rebound (Perkel and Mulloney, 1974). Since the two-cell network is limited to the generation of biphasic motor neuron rhythms, additional network elements would be required for generating polyphasic motor routines, such as the rhythmic movement of articulated limbs or the metachronal contractile wave of serially homologous muscles found in vertebrate and invertebrate locomotion.

Recurrent Cyclic Inhibition

As was apparently first realized by Székely (1965), enlargement of the two-cell network to comprise three or more neurons not only provides for a multiphasic rhythm but also dispenses with the need for fatigue, by opening up the possibility for another source of rhythm generation, namely *recurrent cyclic inhibition.* The oscillatory dynamics of a network with recurrent cyclic inhibition can be readily fathomed from its simplest realization, namely the three-cell oscillator shown schematically in Figure 1a. This network consists of an inhibitory ring formed by three tonically excited neurons (A–C), of which each makes inhibitory synaptic contact with and receives inhibitory synaptic input from one other cell. If, as indicated in Figure 1a, Cell C happens to be in a depolarized, impulse-generating state, its postsynaptic cell, B, must be in a hyperpolarized, inactive state, while its presynaptic cell, A, is recovering from past inhibition. As soon as Cell A *has* recovered from inhibition and reached its impulse generation threshold, Cell C becomes inhibited, thus disinhibiting Cell B and allowing the latter to enter its recovery phase. Once Cell B has recovered, it inhibits Cell A, thus allowing Cell C to begin recovery; and once Cell C has recovered, so that Cell B enters its inactive phase and Cell A its recovery phase, one cycle of the oscillation has been completed. If the time required for recovery from inhibition of each cell is R, and if the time required for establishing inhibition of each cell is small compared to R, then the period, P, of the oscillator cycle

* *Present address:* Department of Biology, University of Virginia Charlottesville, VA 22901, USA

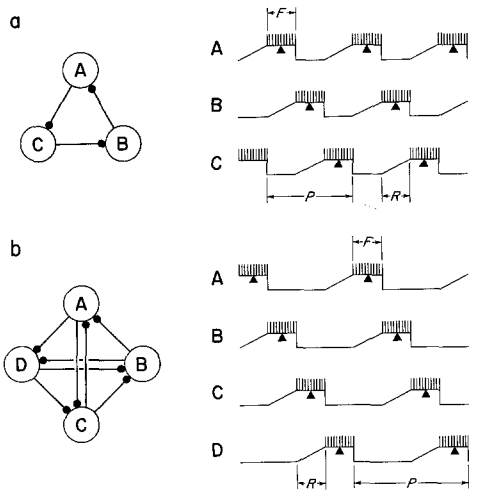

Fig. 1a and b. Simple networks with recurrent cyclic inhibition. **a** Three-cell network. **b** Four-cell network. In this, and all following network diagrams a large circle labeled with a letter or number represents a neuron provided with tonic excitation; filled small circles designate inhibitory synaptic contacts. The traces to the right of each circuit diagram represent the membrane potential and impulse burst activity of individual cells, as determined by theoretical analysis of the network. The triangle points to the midpoint, or middle spike, of an impulse burst

is evidently equal to $3R$. It is to be noted that this oscillatory network gives rise to three activity phases separated by phase angles of 120° and that the cycle phases of the three cells progress in a sense opposite to that of the inhibitory connections forming the ring.

An extensive analytical study by Kling and Székely (1968), of a variety of cyclic inhibition networks has shown that they produce stable oscillations over a broad range of system parameters and can generate as many different cycle phases as the number of cells they contain. Any such ring containing an *odd* number, N, of cells linked in a manner so that every cell makes inhibitory contact with, and receives inhibition from, one other cell will oscillate with a cycle period

$$P = NR. \tag{1}$$

In this N-membered ring, one cell is always in its recovery phase, while the remaining $N-1$ cells form an alternating sequence of active and inactive phases. By contrast, simple rings containing an *even* number of cells do not oscillate, since they can assume one of two stable states, under which either all the even-numbered or all the odd-numbered cells are in the active phase, without any cell being in its recovery phase.

This consideration makes it plain why two-cell networks do not oscillate without a source of fatigue. However, in the case of rings containing four or more cells, topologically more complex networks can be formed, in which recurrent cyclic inhibition does produce an oscillatory activity pattern, even if the number of cells in the ring is even. The simplest (symmetric) realization of such a network is an ensemble of four cells, of which each makes inhibitory contact with and receives inhibition from two other cells (Fig. 1b). As shown by Kling and Székely (1968), in this four-cell network one cell (say Cell A) is in the active phase, the two cells subject to inhibition by that cell (i.e. Cells C and D), are in the inactive phase and the cell subject to inhibition by these two cells (i.e. Cell B) is in the recovery phase. The network gives rise to four activity phases separated by phase angles of 90°, with the period of the oscillator cycle being equal to $4R$. Theoretical analyses of oscillatory neuronal networks with recurrent cyclic inhibition have been made also by Ádám (1968), Pozin and Shulpin (1970), and Dunin-Barkovskii (1970).

The Leech Swimming Rhythm

Recently, the cellular components and synaptic connections of an oscillatory network of interneurons have been identified in the central nervous system of the leech. These interneurons drive the swimming movement of the leech and appear to function in accord with Székely's recurrent cyclic inhibition principle (Friesen et al., 1976). Leeches swim by undulating their extended and flattened body in the dorsoventral plane to form a wave that travels rearwards along the animal. The moving trough and crests of this body wave are produced by a metachronal rhythm of antiphasic contraction-distention cycles of the dorsal and ventral longitudinal muscles in the body wall of each of the 21 abdominal segments. The period of this rhythm varies from about 400 to 2000 ms. In the medicinal leech, *Hirudo medicinalis*, the swimming rhythm has been shown to be controlled by an ensemble of bilateral pairs of excitatory and inhibitory motor neurons present in each of the segmental ganglia of the leech ventral nerve cord. This neuronal ensemble includes excitors (Cells 3, 5, 7, and 107) and inhibitors (Cells 1 and 102) of the dorsal longitudinal muscles, as well as excitors (Cells 4, 8, and 108) and inhibitors (Cells 2 and 119) of the ventral longitudinal muscles. During swimming the membrane potential of these motor neurons oscillates between a depolarized and a hyperpolarized state, with an impulse burst arising during the depolarized state (Ort et al., 1974).

The phases of the rhythms of motor neuron activity, as determined by the timing of the middle impulse of each impulse burst and with the standard phase angle 0° arbitrarily assigned to the rhythm of Cell 3, are approximately 90° for Cell 1, 180° for Cells 4 and 102, and 270° for Cell 2 (Fig. 2). (The other three dorsal excitors, Cells 5, 7, and 107 are active in the same phase

as Cell 3, whereas the other two ventral excitors are active in nearly, but not exactly the same phase as Cell 4. The impulse burst of the more recently identified ventral inhibitor, Cell 119, occurs in a phase of about 0°.) Inasmuch as the time taken for the body wave to travel from head to tail is about equal to the swim period (so that the swimming leech forms one wavelength), the impulse burst phase of each of these motor neurons leads that of its serial homolog in the next posterior segmental ganglion by about 20° (Kristan et al., 1974a). Execution of the swimming movement can, therefore, be accounted for by the activity pattern of this ensemble of identified motor neurons. The motor neurons are not, however, the source of their own activity pattern (Ort, et al., 1974). Instead, the swimming rhythm must be imposed on them by other, oscillatory neural elements. Moreover, since the motor neurons of an isolated leech ventral nerve cord can exhibit sustained episodes of the swimming rhythm, these elements constitute a central oscillator whose multiphasic activity pattern is generated in the absence of peripheral afference (Kristan and Calabrese, 1976).

A search for this central swimming oscillator led to the identification of four bilateral pairs of interneurons, namely Cells 123, 28, 33, and 27, in each of the segmental ganglia, which meet the diagnostic criteria of oscillator components: their membrane potentials oscillate with a period matching that of the swimming rhythm and passage of current into them shifts the phase of the motor neuron activity cycles (Friesen et al., 1976, 1977). The activity cycles of these oscillator interneurons occur in a phase progression, such that the phases of the cycles of Cells 123, 28, 33, and 27 correspond to phase angles of about 0°, 90°, 180°, and 270°, respectively (Fig. 2). Since individual oscillator interneurons are unlikely to possess an endogenous polarization rhythm, their rhythmic activity appears to be the result of an oscillatory neural network (Friesen et al., 1977). This network consists of both intraganglionic and interganglionic synaptic connections of serial homologs of the interneuron quartet. The connections identified thus far are summarized in Figure 3, in which the four hemilateral interneurons of two ganglia—one more anterior and the other more posterior—have been placed at the corners of a square, so that their activity phases progress clockwise. *Intra*ganglionically, three of the interneurons (Cells 33, 28, and 123) make inhibitory connections with the cells that lead them by a phase angle of 90° in the activity rhythm, and two antiphasically active interneurons (Cells 27 and 28) make reciprocally inhibitory connections. Moreover, one interneuron pair (Cells 33 and 28) is linked also via a rectifying electrical junction. Although this is not shown in Figure 3, at least two of the oscillator interneurons are linked via electrical junctions to their

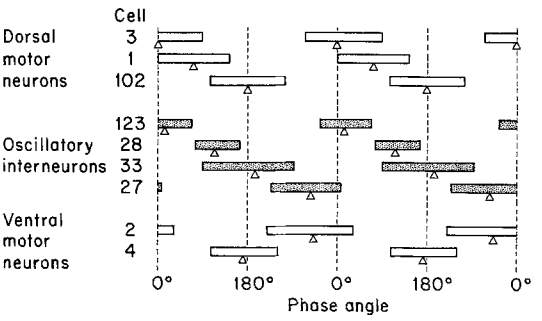

Fig. 2. Phase diagram of the activity cycles of identified motor neurons and interneurons of segmental ganglia of the leech nerve cord during a swimming episode of an isolated preparation. Each bar indicates the duration of the impulse burst of the cell; the triangle under the bar points to the burst midpoint, or middle spike. The burst midpoint of Cell 3 has been arbitrarily assigned the phase angle 0°. (From Friesen et al., 1976; 1977)

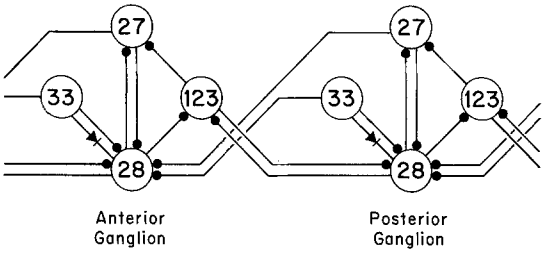

Fig. 3. Summary circuit diagram of identified intra- and interganglionic synaptic connections between the oscillatory interneurons driving the swimming rhythm. The diode represents a rectifying electrical junction. (From Friesen et al., 1977)

contralateral homologs, thus assuring that the activity cycles of left and right segmental oscillators are locked in phase.

*Inter*ganglionically, the three interneurons (Cells 28, 33, and 27) whose axons project into the anterior connective, make inhibitory connections in several more anterior ganglia with the serial homologs of one or both of the cells with which they also connect in their own ganglion. The one interneuron (Cell 123) whose axon projects into the posterior connective, however, makes inhibitory connections in several more posterior ganglia with the serial homologs of the cell that in its own ganglion follows it by a phase angle of 90°. Hence, in contrast to the frontward interganglionic connections, the rearward interganglionic connection has no intraganglionic homolog.

The interneuronal network diagrammed in Figure 3 differs in two respects from that previously presented in the preliminary report (Friesen et al., 1976). First, the network of Figure 3 lacks the intraganglionic inhibitory connection leading from Cell 33 to Cell 123, previously inferred to exist on the basis of indirect evidence. Further experimental observations have made it unlikely that such a connection does, in fact, exist. Second,

the modified network lacks the previously shown direct intra- and interganglionic inhibitory connections leading from Cell 27 to Cell 33. These connections have been omitted from the present schema because the evidence originally secured for their existence is compatible also with the known indirect connections leading from Cell 27 to Cell 33 via Cell 28, as manifest in the schema of Figure 3. Moreover, as will be shown further below, the presence of *direct* intra- or interganglionic inhibitory links from Cell 27 to Cell 33 is not required for generation of the swimming rhythm.

In addition to the network shown in Figure 3, a set of excitatory and inhibitory, intra- and interganglionic connections leading from the oscillator interneurons to the motor neurons has been identified (Poon et al., 1977). These oscillator output connections suffice to account for generation of a good approximation to the observed motor neuron rhythm, lending strong support to the conclusion that the oscillator interneurons are, in fact, the principal components of the central swim oscillator.

The purpose of this paper is to present theoretical arguments, supported by the output data of electronic analog models of neuronal circuits, which show that recurrent cyclic inhibition in the topologically complex network of Figure 3 can indeed account for the generation of the intra- and intersegmental coordinated interneuronal activity pattern characteristic of the leech swimming rhythm.

2. Materials and Methods

Analog Neurons

A complete description of the circuit of the electronic analog neurons, or "neuromimes", used in this study has been published by their designer, Lewis (1968). A previous account of their mode of employ in the simulation of the oscillatory properties of neural networks has been given by Wilson and Waldron (1968). The Lewis neuromimes depend on the articulation of two basic circuits. One circuit represents the analog of an excitable nerve cell membrane, which gives rise to an impulse (i.e., large-amplitude voltage transient) once the membrane polarization has fallen below threshold level, according to the Hodgkin-Huxley theory. The cell membrane analog circuit also provides for the simulation of both excitatory and inhibitory synaptic currents, whose summed effect determines whether the membrane is polarized above or below the impulse threshold level. The output of the cell membrane analog circuit is the simulated membrane potential at the axonal impulse initiation site, and hence reflects both synaptic potentials and impulses. The only adjustable parameter of this circuit is the level of the impulse initiation threshold. The overall function of the cell membrane analog is to integrate continuously the synaptic input, and if membrane polarization falls below threshold, to produce an impulse. A total of eight such cell membrane analog circuits were available for this study. In order to link two of these circuits by the analog of an electrical junction, their output terminals were connected via a resistor. This resistance was chosen to be five times greater than that of the simulated cell membrane resistance, so as to produce a coupling factor of about 0.2. Since the electrical junctions modeled in this work are rectifying, the connections contained a diode in series with the resistor.

The other circuit embodied in the Lewis neuromime represents the analog of a synaptic junction. The synapse analog circuit converts the impulses produced by the cell membrane analog into a signal with the wave form of a synaptic potential, i.e., into a voltage step followed by exponential decay. The synapse analog circuit provides for variation over a wide range of two parameters, namely of the amplitude and of the time constant of decay of the voltage step. In order to model the synaptic coupling of two neurons, the input terminal of a synapse analog circuit is connected to the output terminal of one ("presynaptic") cell membrane analog and the output terminal of the synapse analog is, in turn, connected to either the excitatory or the inhibitory input terminal of another ("postsynaptic") cell membrane analog. A total of 40 synapse analog circuits were available for this study. Tonic excitatory synaptic input to the neuromimes was modeled by connecting the output terminal of a variable frequency pulse generator to the input terminal of a synapse analog circuit and connecting, in turn, the output terminal of the latter to the excitatory synaptic input terminals of the cell membrane analogs. Thus, by changing the output frequency of the pulse generator it was possible to vary simultaneously the level of tonic excitation supplied to all the neuromimes of the network. The frequency of impulse generation resulting from such tonic excitation was determined by the setting of the impulse initiation threshold of the cell membrane analog circuits.

Delay System

Since the neural elements of the network that generates the leech swimming rhythm are distributed over the segmental ganglia of the ventral nerve cord, impulses conducted intersegmentally in the interneuronal axons may require as much as 100 ms to travel from the site of their initiation to the synaptic terminal at the target cell (Poon et al., 1977). To model these conduction times in the oscillatory neural networks to be studied, an impulse delay system was constructed. The input element of this delay system consists of a pulse-shaping circuit which converts impulses received from the output terminal of a cell membrane analog into a square wave pulse compatible with the input requirements of a 1024-bit static shift register [Signetics 2533] driven by a variable frequency clock. Depending on the frequency to which the clock is set, there lapses from 10 ms to 1000 ms between the times that the pulse appears at the input terminal and reappears at the output terminal of the shift register. The output terminal of the shift register is connected to the input terminal of another pulse-shaping circuit, which reconverts the square wave pulse to an impulse signal compatible with the input requirements of a synapse analog. A total of nine such delay systems was available for this study.

Recording Procedures

The output of the cell membrane analog circuits was viewed on an 8-trace oscilloscope and recorded on magnetic tape with an 8-channel FM recorder. The records were later transcribed from tape to paper at a four-fold speed reduction by means of an 8-channel Brush-Gould penwriter. This procedure allows faithful transcription of signals up to about 300 Hz, so that the analog signals of synaptic potentials and impulses can be recorded with rather little attenuation of their amplitude or distortion of their time course, without use of an oscilloscope camera.

3. Results

Variation of the Oscillator Cycle Period

Any neuronal network put forward to account for the generation of the leech swimming rhythm must explain not only how the segmental motor neuron activity

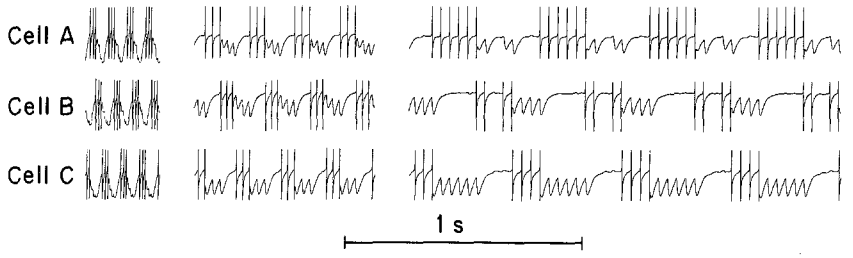

Fig. 4. Variation in the oscillator period. Impulse bursts generated by neuromimes connected according to the three-cell network of Figure 1a, at three different levels of tonic excitation. In the first part of this record, the free running impulse frequencies are about 100 Hz, in the second part about 35 Hz, and in the third part about 25 Hz

pattern and its intersegmental coordination is generated but also how the period of that rhythm can vary over a wide range. As is evident from (1) the period of the oscillations of a network with recurrent cyclic inhibition ought to vary with the recovery time, R, that elapses between the occurrence of the last inhibitory synaptic potential and the first impulse in the activity cycle of each cell. In case the cell membrane responds to voltage transients as a passive element, the value of R is given by

$$R = \varrho_i C_i \ln[V_I - V_E)/(V_T - V_E)], \quad (2)$$

where ϱ_i and C_i are respectively the input resistance and capacitance of the impulse initiation zone of the cell, V_I is the membrane potential after occurrence of the last inhibitory synaptic potential, V_E the steady-state potential to which tonic excitation would depolarize the cell in the absence of inhibition, and V_T is the threshold potential for impulse generation. Provided that for the interneurons of the central swim oscillator ϱ_i, C_i, and V_T have the same value for fast and slow swims and V_I increases with the impulse frequency of the presynaptic neurons supplying inhibitory input to the cell (where $V_I > V_T$), it seems most likely that any increase in R responsible for deceleration of the rhythm is the consequence of a decrease of V_E. That is to say, the longer recovery times responsible for slower swims are likely to be the result of a decrease in the level of tonic excitation of the oscillator cells.

This prediction was tested by means of a model of the three-cell network of Figure 1a. For this purpose, an equivalent electrical analog circuit was constructed, consisting of three electronic analog neurons, or "neuromimes", representing Cells A–C. The impulse threshold of each neuromime was set to a constant value, V_T and the frequency of the pulse generator supplying tonic excitatory input to it (and hence V_E) was varied systematically while leaving all other network parameters constant. The step amplitude (and hence V_I) and time constant of exponential decay of the inhibitory synaptic potentials produced at the synaptic junction analogs linking the neuromimes (and hence $\varrho_i C_i$) were set such that at all levels of tonic excitation employed the impulse rate of each presynaptic cell sufficed to bring the postsynaptic cell below its impulse threshold and that upon cessation of impulse activity in the presynaptic cell the postsynaptic cell resumed its own impulse activity within the realistic time range of $R = 50$ to 250 ms after receipt of the last inhibitory synaptic potential.

Figure 4 presents the output of the three neuromimes of this analog circuit for three decreasing levels of tonic excitation, and hence for three different levels of V_E, corresponding to steady-state impulse frequencies of 100, 35, and 25 Hz. As can be seen, the cycle period shows the expected increase, from about 80 ms through 190 ms to about 450 ms. Moreover, it is clear that this more than 5-fold increase in cycle period is accounted for by a corresponding progressive increase in R. Since the duration F of the impulse burst phase of each cell of the three-cell network is equal to R (Kling and Székely, 1968), F similarly increases with any increase in the cycle period. The number of impulses per burst ought to be nearly independent of the period, because any increase in F is compensated by a corresponding decrease in the impulse frequency during the impulse burst. As can be seen in Figure 4 the output of the analog circuit also meets this expectation over the 5-fold range of cycle periods.

Intersegmental Impulse Conduction Delays

As will be seen in the following, the oscillatory activity of the interneuronal network of the central swim oscillator depends critically upon the fact that Cells 28, 33, and 27 of a given ganglion make their inhibitory connections not only with their correspondent interneurons of the very next anterior ganglion but repeat these connections with the serially homologous interneurons of several successive anterior ganglia. Similarly, Cell 123 of a given ganglion forms an inhibitory connection with the serial homologs of Cell 28 in several posterior ganglia. Although, because of technical limitations, this segmental iteration of interganglionic inhibitory connections between oscillator interneurons has been identified directly only for the next and the next-but-one ganglion, the finding that the interneurons form iterated connections with motor neurons for at least five segments to the front (or, in the case of Cell 123, two segments to the rear) makes it seem

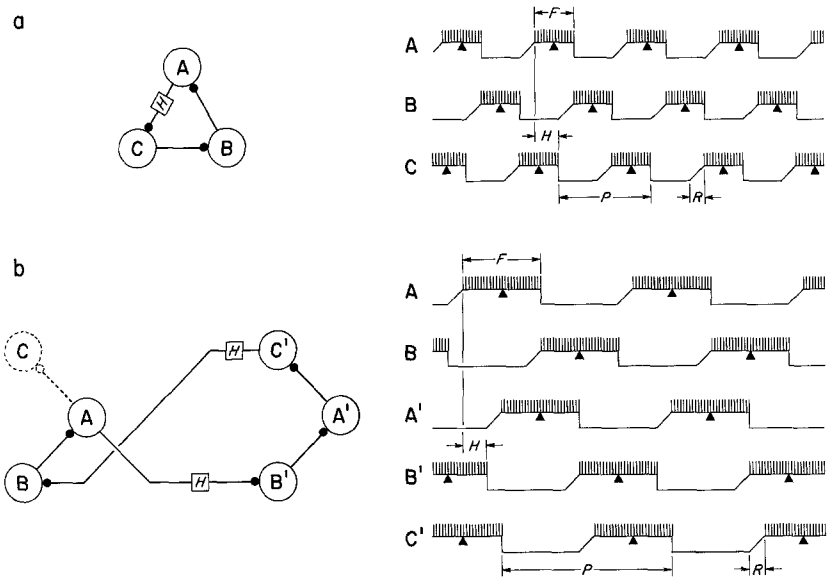

Fig. 5a and b. Recurrent cyclic inhibition networks with transmission delays. **a** Three-cell network with one transmission delay. **b** Five-cell network with two transmission delays. Cells A, B, and C represent the neurons of an anterior ganglion and Cells A′, B′, and C′ their homologs of a posterior ganglion. The stippled Cell C lies outside the ring. The squares enclosing the letter *H* identify connections with transmission delays

likely that the connections between interneurons are also repeated for at least five segments (Friesen et al., 1976, 1977). Thus it appears that the cord-wide ensemble of segmental oscillators is very extensively interlocked. Since impulses conducted frontward or rearward in the intersegmental axons of the interneurons take about 20 ms to travel from one ganglion to the next, the segmentally interlocked interneuronal network incorporates some connections in which delays of up to 100 ms intervene between the generation of an impulse in the presynaptic cell and appearance of a synaptic potential in the postsynaptic cell.

In order to assess the effect of such impulse conduction delays on the activity rhythm of recurrent cyclic inhibition networks, we first consider the modification of a simple three-cell network, shown in Figure 5a. This network has exactly the same properties as that shown in Figure 1a, except that here the inhibitory connection from Cell A to Cell C incorporates a fixed, period-independent impulse conduction time *H*. The graphical analysis of Figure 5a of the effect of this additional delay element shows that its presence increases the cycle period to the value

$$P=3R+2H. \tag{3}$$

By extension of this analysis to an *N*-membered ring with *N* inhibitory connections, of which *M* each embody a delay *H*, the cycle period is found to be

$$P=NR+2MH. \tag{4}$$

Comparison of (1) and (4) indicates that introduction of a fixed impulse conduction delay into the recurrent cyclic inhibition network causes the cycle period to take on a *constant time* sector, namely $2MH$, in addition to the *variable time sector* NR.

Analysis of the three-cell network with delay shows, furthermore, that the phase angle by which the beginning of the active phase of Cell C precedes that of Cell A is 360° R/P, whereas the corresponding phase angle by which the cycle of Cell A leads that of Cell B and by which the cycle of Cell B leads that of Cell C is 360° $(R+H)/P$. Evidently, these phase angles are not only unequal but vary in an opposite sense with increases in the period. As the period increases from its minimum of $P=2H$ (for $R=0$) to $P=3R$ (for $R \gg H$), the phase angle by which Cell C leads Cell A *increases* from 0° to 120°, whereas the phase angle by which Cell B leads Cell C and Cell A leads Cell B *decreases* from 180° to 120°. It can be concluded, therefore, that in a cyclical inhibition network containing an invariant impulse conduction time of magnitude comparable to the variable recovery time, the cycle period consists of a variable and a constant time sector. Moreover, in the case of the asymmetrical distribution of the conduction times over the ring of inhibitory connections, changes in the cycle period give rise variations in the individual cycle phase relations.

The Five-Cell Network

We may now consider the simple version of an *inter*segmental oscillatory network with variable period and significant impulse conduction delays shown in Figure 5b. This is a five-cell cyclic inhibition network, consisting of Cells A and B representing the neurons of an anterior ganglion, Cells A′ and B′, representing the homologs of Cells A and B in a posterior ganglion, and Cell C′ representing a cell of the posterior ganglion, whose anterior homolog, Cell C, is considered as lying outside the ring. Together with Cells A and B, Cell C

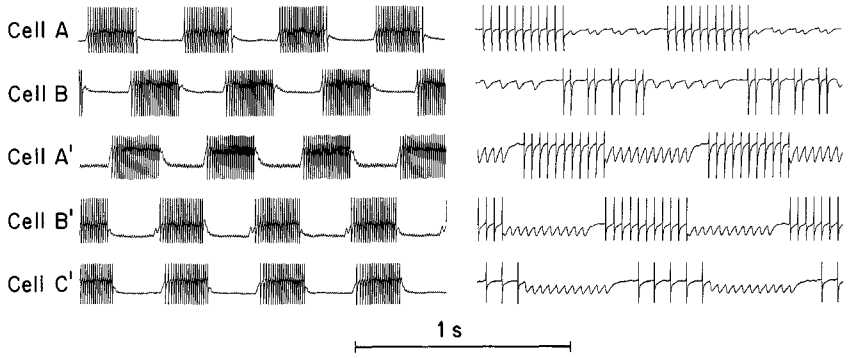

Fig. 6. The interganglionic five-cell oscillator. Impulse bursts generated by five neuromimes connected according to the network of Figure 5b, at two different levels of tonic excitation, with impulse conduction delays of $H = 80$ ms. The free-running impulse frequencies are about 100 Hz for the left-hand and 30 Hz for the right-hand traces

forms part of another ring having homologs in a yet more anterior ganglion as its members. The rearward connection from Cell A to Cell B′ and the frontward connection from Cell C′ to cell B both incorporate impulse conduction delays of length H. In accord with (4) the cycle period of the cells of this network would be expected to be

$$P = 5R + 4H. \tag{5}$$

Moreover, by an extension of the analysis of the three cell network, it can be readily shown for the *intra*ganglionic phase relations of this five cell network that the cycles of Cells A and A′ lead those of Cells B and B′ respectively by a phase angle of 360° $(2R + 2H)/P$, as does the cycle of Cell C′ lead that of Cell A′.

As far as the *inter*ganglionic phase relations are concerned, the cycles of the anterior Cells A and B lead those of their posterior homologs, Cells A′ and B′, by a phase angle of 360° $(R + H)/P$. Thus, over the range of short periods $(R \ll H)$ to long periods $(R \gg H)$ the intraganglionic phase lead of Cells A and A′ over Cells B and B′ decreases from a maximum value of 180° to a minimum value of 144°, whereas the *inter*ganglionic phase lead of Cells A and B over Cells A′ and B′ decreases from a maximum value of 90° to a minimum value of 72°. Since, as can also be shown readily, here the duration F of the impulse burst phase of each cell is equal to $2R + 2H$, the progressive decrease in impulse frequency due to decreases in V_E is not fully compensated by corresponding increases in F, at least until V_E has fallen to levels for which $R \gg H$. Hence, unlike in the network without impulse conduction delays, the number of impulses per burst of each cell in the network with delays is not independent of the level of tonic excitation but decreases with increasing cycle period.

These theoretical predictions were tested by means of an electronic analog circuit constructed according to the schema of Figure 5b. The model consisted of five neuromimes, with two non-adjacent inhibitory connections containing a shift register delay element mimicking an impulse conduction time between four segments of $H = 4 \times 20 - 80$ ms. As was done in the case of the symmetric three-cell circuit without conduction delays, the tonic excitation provided to the neuromimes was varied systematically, while leaving all other network parameters constant. Figure 6 presents the output of the five neuromimes of this analog circuit for two different levels of tonic excitation, or of V_E, corresponding to steady state impulse frequencies of 100 Hz and about 30 Hz. (At the lower tonic excitation level the neuromimes did not all produce the same steady state impulse frequencies, because of the large effect exerted by small variations in the individual settings of V_T on the difference $V_T - V_E$.) As can be seen, at the higher tonic excitation level, when R has the value of about 30 ms, the cycle period of the cells in the five-cell network is about 470 ms, in agreement with the value of $P = (5 \times 30) + (4 \times 80) = 470$ ms estimated from (5). At the lower tonic excitation level, when R has the value of about 120 ms, the cycle period has risen to about 970 ms, in agreement with the estimated value of $P = (5 \times 120) + (4 \times 80) = 920$ ms. At the higher tonic excitation level, the interganglionic delay between the onset of the active periods of Cell A and Cell A′, or of Cell B and Cell B′, is about 115 ms, equivalent to a phase angle of 360°(115/470) = 88°. At the lower tonic excitation level that interganglionic delay rises to about 230 ms, equivalent to a phase angle of 360°(230/970) = 86°. The intraganglionic delay between onset of the active phases of Cell A and Cell B, or Cell A′ and Cell B′, is about 220 ms at the higher level of tonic excitation and about 420 ms at the lower of tonic excitation, corresponding respectively to phase angles of 360°(220/470) = 170° and 360°(420/970) = 160°. Thus both the magnitude and the period-dependence of the inter- and intraganglionic phase delays of the analog model circuit match the theoretical expectations calculated above.

These theoretical considerations account for the observation that the phase relations of the leech swimming cycle during fast and slow swims are not, in fact, independent of the period. For instance, the phase angle by which the impulse burst midpoints of the dorsal excitor, Cell 3, lead those of the ventral excitor,

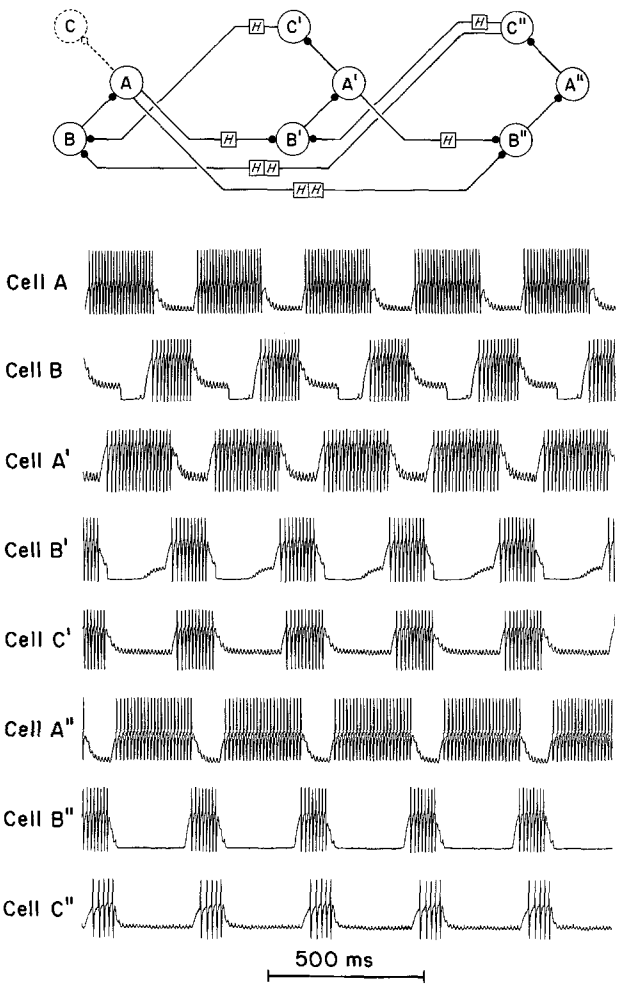

Fig. 7. Two intersegmentally concatenated five-cell networks containing direct interganglionic connections between cells of the outer ganglia that jump the intermediate ganglion. Impulse bursts generated by eight neuromimes connected according to the network shown in the insert. The impulse conduction delay H is 40 ms and the free-running impulse frequency about 100 Hz

Cell 4, increases from about 180° to about 220°, as the swim cycle period increases from 500 to 1250 ms. (Kristan et al., 1974b; Kristan and Calabrese, 1976.) This variation of the cycle phase relations with the period P was previously explained by the inference that the cycle of the segmental swim oscillator consists of a constant time sector lasting about 300 ms and a variable time sector whose changes in length are responsible for the variations in the period (Kristan et al., 1974a, b).

Finally, also in accord with theoretical expectation, the number of impulses per burst during the active phase of each cell decreased with increasing cycle period. Whereas at the higher level of excitation, each neuromime produced slightly more than 20 impulses per burst, at the lower level of excitation neuromimes A, A′, and B′ produced about half the previous number and neuromimes B and C′ about one-third the previous number of impulses per burst. (This difference between the individual neuromimes is unrelated to their position in the network and merely reflects the failure to achieve perfect equality in the adjustment of system parameters.)

Concatenation of Five-Cell Networks

The actual intersegmental connections between the interneurons of the central swim oscillator are more complex than those of the 5-cell network shown in Figure 5b. In particular, the interneurons are linked intersegmentally in a manner such that individual cells may receive inhibitory input from the serial homologs of their presynaptic cells in as many as five anterior or five posterior ganglia. In order to take account of the effect of such multisegmental input to individual oscillator interneurons, we consider the concatenated eight-cell circuit diagrammed in Figure 7. Here Cells A, B, A′, B′, C′ and Cells A′, B′, A″, B″, and C″ form two serially homologous intersegmental five-cell networks, linked via the joint participation of Cells A′ and B′ in both the anterior and the posterior oscillator circuits. However, the networks are linked also via direct intersegmental connections from Cell A to Cell B″ and from Cell C″ to Cell B that jump Cell B′ of the middle segment. Thus, here the serial homologs Cells B, B′, and B″ all receive multisegmental inhibitory input. Theoretical analysis of the mode of operation to be expected of this concatenated network reveals that its overall cycle period is given by

$$P = 5R + 6H, \tag{6}$$

where H is the intersegmental impulse conduction time between Cells A and B′, A′ and B″, C′ and B, or C″ and B′, and $2H$ the conduction time between Cells A and B″, or C″ and B. Comparison of (5) and (6) shows that concatenation increases the cycle period of the network. Moreover, it is to be noted that concatenation introduces an asymmetry into the impulse burst duration, F, of the cells of the network. Whereas, as previously shown, in the simple five-cell network the impulse burst duration has the uniform value $F = 2R + 2H$, in the concatenated network the impulse burst duration varies from $F = R + 2H$ for Cells B″ and C″, through $F = 2R + 2H$ for Cells B, B′, and C′ and $F = 2R + 4H$ for Cells A and A′, to $F = 3R + 4H$ for Cell A″, Thus the concatenation brings an even greater degree of verisimilitude to the output of the five-cell network, since, as can be seen in the phase diagram of Figure 2, the actual impulse burst durations of the four oscillatory interneurons are of significantly different lengths.

Figure 7 presents the output of an analog circuit constructed according to this schema. The model consisted of eight neuromimes. Shift registers were

included in the connections representing intersegmental links, to produce a value of $H=40$ ms appropriate for the impulse conduction time over a distance of two segments. Sufficient tonic excitation was provided to all neuromimes to produce steady state impulse frequencies of about 100 Hz, and values of R of about 30 ms. As can be seen, the model ran with a cycle period of 350 ms, in good agreement with the value of P predicted by (6), namely $P=(5\times 30)+(6\times 40)=390$ ms. Moreover, the individual impulse burst durations manifest just the asymmetry predicted by the theoretical analysis.

The relatively simple five-cell cyclic inhibition network with two fixed delay lines can thus provide a first approximation to the basic operating mode of the leech central swimming oscillator: two interneurons of each ganglion show a roughly antiphasic activity rhythm, whose period can vary over a range of 400–1000 ms and the activity cylces of serial homologs of these interneurons in different ganglia of the nerve cord show a rostro-caudal phase lead of about $80°/4=20°$ per segment. In principle at least, a system of such intersegmentally iterated, concatenated five-cell rings in the ganglia of the abdominal nerve cord would thus be capable of generating a rearward traveling body wave, formed by antiphasic contractions of the segmental dorsal and ventral longitudinal musculature.

The Identified Interneuronal Network as an Oscillator

The preceding theoretical considerations of the five-cell network can now aid us in the analysis of the mode of operation of the identified network of interneurons presented in Figure 3. This network is topologically too complex to permit immediate recognition of its oscillatory features and straightforward explanation of how it manages to generate the observed swimming rhythm. Hence, in order to fathom the modes of operation of the identified network, we begin its analysis by considering the simplified version shown in Figure 8. This schema views the interneurons as forming a five-cell recurrent cyclic inhibition ring, similar to that shown in Figure 5b. For this purpose Cells A, B, and C of Figure 5b are taken to be the equivalents of Cells 123, 28, and 27, respectively, in the anterior ganglion *Y*, and Cells A′, B′, C′ the equivalents of Cells 123, 28, and 27 in the posterior ganglion *Z*. Cell 33 has been added to the circuit as a follower of Cell 28, in both ganglia, subject to periodic hyperpolarization from Cell 28 via the rectifying electrical junction. Cell 27 of the anterior ganglion is a follower of Cell 123, and similarly outside the cyclic inhibition ring. Thus in this circuit, Cell 33 in both ganglia and Cell 27 in the anterior ganglion have no influence on the basic oscillatory properties of the circuit. The output of an electronic analog circuit constructed according to this schema is presented in

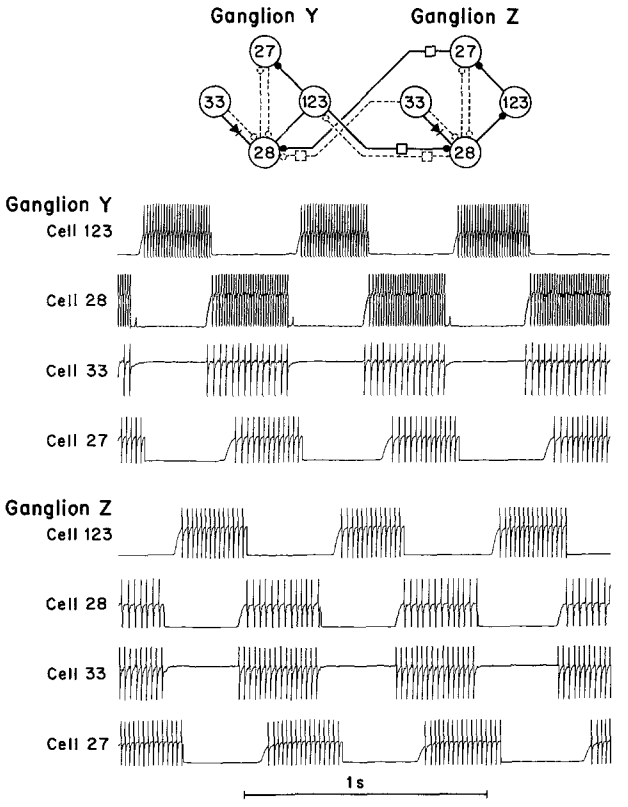

Fig. 8. Oscillation of a reduced version of the interneuronal network of Figure 3, equivalent to a five-cell, recurrent cyclic inhibition ring. Impulse bursts generated by eight neuromimes connected according to the network formed by connections and elements drawn in solid lines in the circuit diagram shown in the insert. In this and the following diagrams, connections and elements drawn in dashed lines have been omitted from the analog circuits. $H=80$ ms. The free-running impulse frequency is about 80 Hz

Figure 8. As expected, the rhythm generated by this network is essentially similar to that generated by the network of Figure 5b. The main realistic features of the simplified network of Figure 8 are that the activity rhythms of Cells 123 and 33 are antiphasic and that the duty cycle of anterior interneuron homologs lead in phase that of posterior homologs. However, as is evident by comparison of Figure 8 with Figure 2, neither the relative phase angle nor the duration of the impulse bursts of Cells 28 and 27 are realistic.

Before analyzing the interneuronal network at higher levels of complexity we must take account of possible differences in the relative strengths of the synaptic connections. Up to this point of our discussion all inhibitory connections were implicitly taken to be *major*, in the sense that for a major connection an impulse burst of the presynaptic cell suffices to polarize the postsynaptic cell beyond the impulse generation threshold potential V_T. However, in the following analysis it will be necessary to consider also *minor* connections, in the sense that for such a minor con-

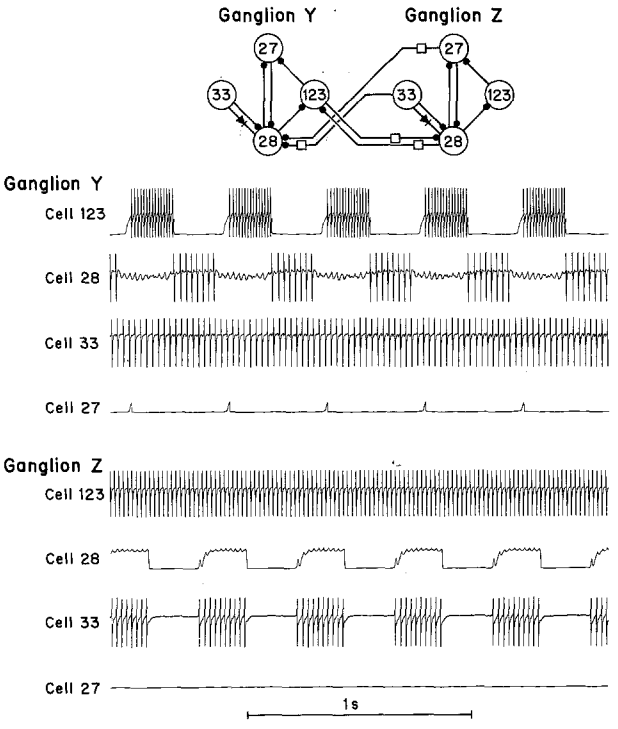

Fig. 9. Oscillation of the full interneuronal network of Figure 3 in two interconnected ganglia, Y and Z, of which Z is the rearmost of the chain. Impulse bursts generated by eight neuromimes connected according to the circuit shown in the insert. The intraganglionic inhibitory connection from Cell 33 to Cell 28 is major in ganglion Z and minor in ganglion Y. All other connections are major. The rectifying electrical junction between Cells 33 and 28 is adjusted to be of such a strength that all major inhibitory inputs to Cell 28, except that provided by Cell 33 itself and its homologs, polarize Cell 33 beyond the impulse threshold potential. $H = 80$ ms. The free-running impulse frequency is about 80 Hz

nection an impulse burst of the presynaptic cell does *not* suffice to polarize the postsynaptic cell beyond threshold potential. Such minor connections can play two different roles in the oscillatory network: a) via a minor connection the activity of a presynaptic cell can increase the recovery time, R, of a postsynaptic cell, by reducing the value of V_E of (2); and b), via minor connections concurrent activity of two or more presynaptic cells can cooperate in bringing a common postsynaptic cell beyond threshold potential. In no case of an identified connection of the leech oscillatory network has it been possible so far to ascertain that it is, in fact, major, although, as will be seen, in one case the available evidence indicates that a connection must be minor. Nevertheless, with the exception of that case, all other identified connections will continue to be considered in the following as being of the major type.

Moreover, it is necessary to address the question of the strength of the rectifying electrical junction linking Cells 33 and 28. For the purpose of the following analysis it will be assumed that the strength of this junction is sufficient to allow input from any *major* inhibitory connection leading to Cell 28 to polarize also Cell 33 beyond its impulse threshold potential. Thus any major inhibitory connection leading to Cell 28 is also a major inhibitory connection, albeit indirect, to Cell 33. However, it will be necessary to assume that polarization of Cell 28 by intraganglionic inhibitory input recieved from Cell 33 itself, or by interganglionic inhibitory input received from posterior homologs of Cell 33, does not polarize Cell 33 beyond threshold potential.

We may now consider the interneuronal network at its full level of topological complexity presented in Figure 3. If all the identified connections shown in that schema are major, the network is not oscillatory: evidently the network can assume a non-oscillatory, stable state under which both homologs of Cell 123 and the anterior homolog of Cell 33 are permanently active and all other cells are permanently inactive. However, it appears inescapable that the intraganglionic inhibitory connection from Cell 33 to Cell 28 is, in fact, minor, since the phase diagram of Figure 2 indicates that the impulse burst of Cell 28 occurs while Cell 33 is itself active. It seems likely that the reduced efficacity of the inhibitory connection leading from Cell 33 to Cell 28 is attributable to the presence of the rectifying electrical junction, which allows passage of depolarizing current from Cell 33 to Cell 28 while Cell 33 is hyperpolarizing Cell 28 via inhibitory synaptic potentials. Nevertheless, even if the necessarily minor character of the intraganglionic link from Cell 33 to Cell 28 is taken into account, the network of Figure 3 still does not oscillate. With this modification the network can assume a non-oscillatory stable state under which the posterior homologs of Cells 33 and 28 and the anterior homolog of Cell 27 are permanently active, and all other cells are permanently inactive. To allow the network to oscillate, it is necessary to posit an exceptional situation in the rearmost ganglion, Z, of the chain. This exceptional situation concerns the link between Cells 33 and 28, whose inhibitory component would be major, in the sense that during its active phase Cell 33 can hyperpolarize Cell 28 beyond threshold potential level. At the same time, the link would still be minor in that it does not produce enough hyperpolarization of Cell 28 to cause sufficient return flow of hyperpolarizing current via the rectifying electrical junction to polarize Cell 33 itself beyond threshold potential level. Although the postulation of this exceptional situation in the rearmost ganglion is admittedly ad hoc, it can be rationalized by the finding that the swimming rhythm appears to be driven by a source of excitation reaching ganglia from the rear (Poon, 1976) and that, accordingly, Cell 28 in any rearmost ganglia would be deprived of that excitatory source and hence

more readily subject to polarization beyond impulse threshold by the minor inhibitory input reaching it from Cell 33. In any case, once this further elaboration is taken into account, the full network shown in Figure 3, does produce stable oscillations. It is now formally equivalent to a three-cell cyclic inhibition network with two conduction delays, constituted by Cells 123 and 28 of the anterior ganglion Y and Cell 33 of the rearmost ganglion Z, and, in accord with (4), oscillates with a period $P=3R+4H$. The nature of these oscillations can be seen in the output of the electronic analog circuit presented in Figure 9. Evidently, the interneuronal activity pattern produced by this network bears little resemblance to the swimming rhythm. Only three of the eight cells are rhythmically active, while of the remainder, two are permanently active and three are permenantly inactive. As far as its realism is concerned, the output of this full network is clearly inferior to that of the reduced network of Figure 8.

But if we consider the concatenation of three rather than two full interganglionic networks, we encounter a system that produces stable oscillations with a period $P=4R+6H$ and whose rhythm is more realistic than that of the reduced five-cell circuit of Figure 8. As is evident from the output of a neuromime analog circuit representing the three ganglia shown in Figure 10, the rhythms of Cells 123, 28, and 27 of the frontmost ganglion X now occur in a realistic phase relation, with the major still remaining defect of the output being the precocious onset of the Cell 33 impulse burst in ganglion X. The finding that the two other ganglia, Y and Z, of this concatenated network do not produce an appropriate swimming rhythm is not, however, to be considered a defect. On the contrary, it has been observed that the rearmost ganglia of an intact leech ventral nerve cord do not, in fact, manifest the swimming rhythm (Kristan et al., 1974b). Moreover, it has also been observed that an isolated nerve cord produces the swimming rhythm only if it consists of a chain of at least six or more ganglia. Hence, the results of this analysis suggest that proper function of the central swim oscillator requires the presence of some posterior "edge" ganglia which provide rhythmic input to anterior ganglia, without themselves undergoing the full swim rhythm.

Finally we examine one further elaboration of the network, in order to generate a more realistic duty cycle of Cell 33. For this purpose we add the oscillatory interneurons and their connections of one more ganglion to the three-ganglion circuit of Figure 10 and consider the operation of the concatenated chain of four ganglia. The significant differences that exist between the modes of operation of the three-ganglion and four-ganglion networks are attributable mainly to the influence of the (major) frontward inhibitory connections leading from Cell 27 to anterior homologs of Cell 28. Since the Cell 27 homologs in the two posterior ganglia, Y and Z, are permanently inactive, their frontward connections are of no consequence for the operation of the three-ganglion network. However, since Cell 27 of ganglion X *is* rhythmically active, its frontward connection to Cell 28 of ganglion W *can* make a contribution to the operation of the four-ganglion network. Unfortunately, a lack of sufficient neuromime elements prevented the construction of an electronic analog of the entire four-ganglion network. However, theoretical analysis of its mode of operation gave the result presented in Figure 11. Evidently, the activity pattern of the interneurons of the posterior two ganglia, Y and Z, bears no greater resemblance to the swimming rhythm in the four-ganglion network than it does in the three-ganglion network. By contrast, the interneurons of the anterior ganglia, W and X, of the four-ganglion chain do show a greater realism, as indicated by comparison of the results of the theoretical analysis with the phase diagram of Figure 3. In

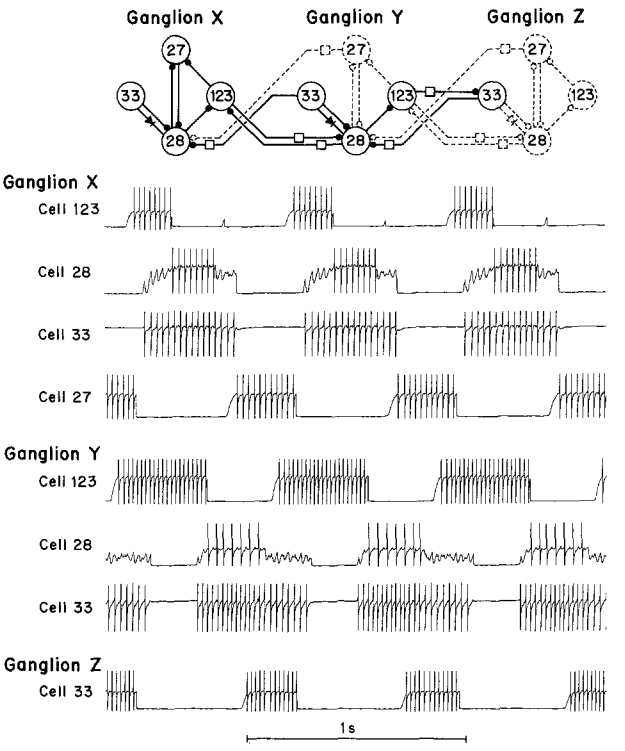

Fig. 10. Oscillation of the full interneuronal network in three ganglia, X, Y, and Z. Impulse bursts generated by eight neuromimes connected according to the circuit shown in the insert. Neuromimes representing the non-oscillatory Cells 28, 123, and 27 of the rearmost ganglion Z and the non-oscillatory Cell 27 of the middle ganglion Y have been omitted from the circuit, since they make no contribution to the rhythm generation. The indirect major connection of Cell 123 of ganglion Y to Cell 33 of ganglion Z via Cell 28 has been replaced without loss of verisimilitude by a direct, major inhibitory link. $H=80$ ms. Free running impulse frequency about 80 Hz

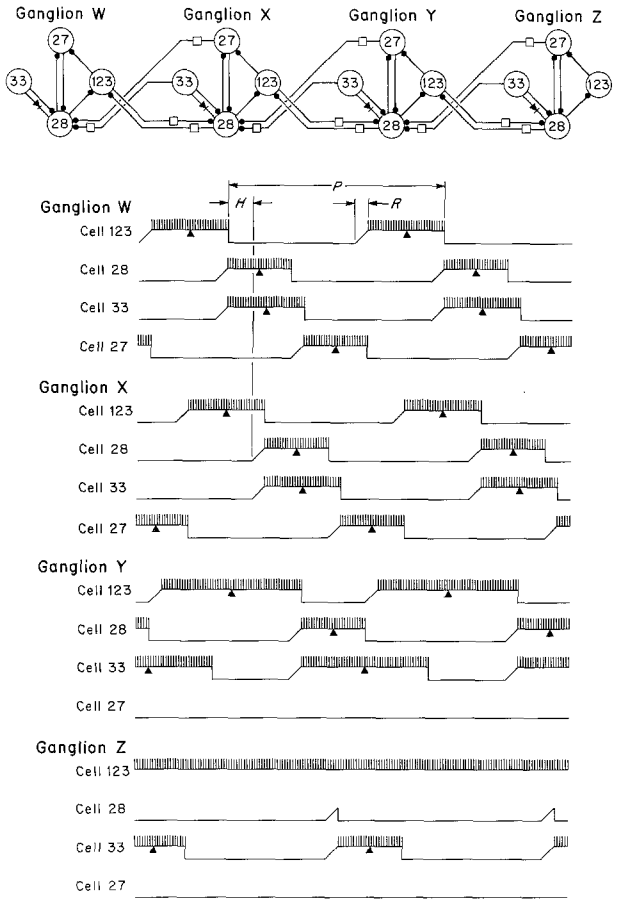

Fig. 11. Theoretical analysis of the operation of the full interneuronal network in a chain of four isolated ganglia, W, X, Y, and Z. $P=5R+6H$

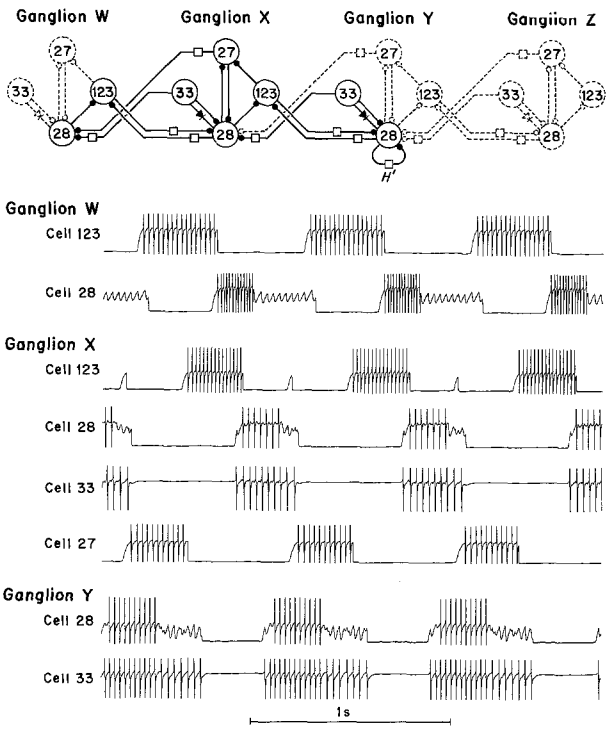

Fig. 12. Oscillation of a partial electronic analog model of the full interneuronal network in four ganglia, W, X, Y, and Z, representing the 1st, 5th, 9th, and last of an isolated chain of 13 ganglia. Impulse bursts generated by eight neuromimes connected according to the circuit shown in the insert. The delay H' in the self-inhibitory "phantom" connection of Cell 28 in ganglion Y was set to 250 ms. $H=80$ ms. Free-running impulse frequency about 80 Hz

particular, the impulse bursts midpoints of the four interneurons now occur in an appropriate phase relation. Addition of the fourth ganglion also lengthens the cycle period of the oscillation to $P=5R+6H$, from the value $P=4R+6H$ for oscillation of the three-ganglion network.

In order to confirm the essential validity of the theoretical analysis of the four-ganglion network, a partial electronic analog model was constructed with the eight available neuromimes. This analog circuit incorporated Cells 123 and 28 of the frontmost ganglion W, Cells 123, 28, 33, and 27 of ganglion X, and Cells 123 and 28 of ganglion Y. To simulate the rhythmic inhibitory input which Cell 28 of ganglion Y receives from Cell 33 of the rearmost ganglion Z, Cell 28 of ganglion Y was connected to itself via an inhibitory connection that incorporated a delay $H'=2H+R$, or the time normally elapsed between the onset of the impulse burst of Cell 28 of ganglion Y and its receipt of the first inhibitory synaptic potential due to the onset of the impulse burst of Cell 33 of ganglion Z. Thus this "phantom" connection replaces the cells that constitute the posterior three-cell recurrent cyclic inhibition subnetwork, namely Cell 123 of ganglion Y and Cells 33 and 28 of ganglion Z. The absence of any of the other cells that were omitted from the partial network should not have any significant consequence for the duty cycles of the four interneurons of ganglion X. As can be seen from the output of this partial model network presented in Figure 12, the four neuromimes representing Cells 123, 28, 33, and 27 of ganglion Y do produce an activity rhythm with reasonably realistic duty cycles. Thus the results of the theoretical analysis of the entire four ganglion network presented in Figure 11 appear to be essentially correct.

4. Discussion

The preceding theoretical considerations thus show that Székely's principle of recurrent cyclic inhibition allows the identified interneural network of the segmental ganglia of the leech shown in Figure 3 to generate stable oscillations. However, because of an "edge effect" of the rearmost ganglion of any chain of ganglia a minimum chain length of four ganglia is required for

generation of interneuronal activity cycles appropriate for the swim rhythm. This conclusion is in harmony with the finding that an isolated leech ventral nerve cord exhibits swim episodes only if it consists of a chain of at least six or more ganglia (Kristan and Calabrese, 1976). In addition to being capable of generating a swim rhythm with realistic cycle period and intra- and intersegmental phase relations, the concatenated recurrent cyclic inhibition network also responds to a decrease in the general level of tonic excitation of the interneurons with a proportional increase in the length of the period and the front-to-rear intersegmental delay between impulse bursts of serially homologous interneurons that is appropriate for the swimming movement.

Paradoxically, this last fact might seem to weigh *against* the conclusion that the identified network is the central swim oscillator, since the approximately linear increase of the intersegmental swim cycle delay with the period that causes the leech to maintain one wavelength of the body wave during both fast and slow swims, has so far been observed only with *intact* preparations not deprived of sensory input (Kristan et al., 1974a). By contrast a period-independent intersegmental phase lag is not generally manifest in recordings taken from serially homologous motor neurons in successive ganglia during progressively longer cycle periods of swimming episodes of an *isolated nerve cord.* As Kristan and Calabrese (1976) found, a plot of the delay between impulse bursts of serially homologous motor neurons against the observed cycle period produces widely scattered points. Because of that wide scatter, it is difficult to abstract from such a plot the linear increase of delay with cycle period demanded by the invariant intersegmental phase lag of the swimming rhythm. Fortunately, the recurrent cyclic inhibition mechanism of rhythm generation put forward here is able to provide an explanation of this puzzling aspect of recordings taken from isolated nerve cord preparations. For this purpose, we may envisage that the level of tonic excitation, and hence the difference $V_T - V_E$, and hence the value of R, is subject to considerable fluctuations in individual oscillator interneurons. The effect of such individual fluctuations of the value of R on measurements of the intersegmental phase delay as a function of cycle period at different *average* levels of tonic excitation can now be considered in terms of the simple 5-cell network of Figure 5b. If for each of the five cells the actual value of R differs from the average value R of the network by $r_A, r_B, r_{A'}, r_{B'}$, and $r_{C'}$, then the period is given by

$$P = R + r_A + R + r_B + R + r_{A'} + R + r_{B'} + R + r_{C'} + 4H\,. \quad (7)$$

But since $r_A + r_B + r_{A'} + r_{B'} + r_{C'} = 0$, it is still true that

$$P = 5R + 4H\,. \quad (5)$$

However, the delay between the impulse bursts of Cell A and of its posterior homolog Cell A′ is given by

$$D(A \rightarrow A') = H + R + (r_{A'} + r_{B'})/2\,. \quad (8)$$

That is to say, whereas, regardless of the magnitude of individual fluctuations, the cycle period of the network depends only on the average value of R, the intersegmental phase delay between serial homologs does vary with the deviation of individual values of R from that average.

The recurrent cyclic inhibition model of the central swim oscillator presented here has the further advantage that its basic mode of operation is reasonably independent of the exact magnitudes of network parameters. The model produces stable oscillations as long as the intersegmental impulse conduction delay, H, exceeds the recovery time R, all inhibitory connections (except that leading from Cell 33 to Cell 28) are "major", and the tonic excitation of the interneurons is sufficiently high to allow each presynaptic cell to polarize its postsynaptic cell beyond impulse generation threshold. The only network parameters that do require a more delicate adjustment pertain to the link between Cells 33 and 28. Here the strength of the rectifying electrical link, the relative level of the impulse generating thresholds of the two cells and the amplitude of the inhibitory synaptic potentials delivered by Cell 33 to Cell 28 must be so matched that any major inhibitory input to Cell 28, other than that provided by Cell 33 homologs, also hyperpolarizes Cell 33 beyond the impulse threshold potential, while hyperpolarization of Cell 28 caused by activity of Cell 33 and its homologs does not polarize Cell 33 beyond threshold.

However complex the identified network diagrammed in Figure 3 may appear, it is unlikely that the central swim oscillator is actually of a lesser complexity. As experiments with the electronic analog model circuits have shown, every intra- and interganglionic connection included in the diagram appears to be necessary for the generation of stable oscillations resembling the actual swimming rhythm. Removal of any one major connection from the network immediately stops its oscillation. One exception is the intraganglionic connection leading from Cell 27 to Cell 28, upon the removal of which the oscillation decays gradually. The network can, of course, resume oscillation if several major connections are removed from it simultaneously, as was done in the case of the five-cell ring network of Figure 8. But here the oscillation lacks the appropriate phase relations. In fact, rather than being overconnected, the network of Figure 3 probably does not yet show the central swim oscillator in its full complexity, in that some of its elements responsible for fine tuning may not have been found as yet. Nevertheless, it seems likely that the basic skeleton of

the central swim oscillator of the leech has been identified and that the network owes its oscillations to the recurrent cyclic inhibition mechanism.

Acknowledgements. We are indebted to Donald Kennedy for providing us with neuromime elements. This work was supported by NIH Research Grants GM 17866 from the Inst. of General Medical Sciences, and NS 12818 from the Inst. of Neurological Diseases and Stroke, and BNS 74-24637 A 02 from the National Science Foundation; and by NIH Postdoctoral Fellowship NS 05144 from the Inst. of Neurological Diseases and Stroke.

References

Ádám, A.: Simulation of rhythmic nervous activities. II. Mathematical models for the function of networks with cyclic inhibition. Kybernetik **5**, 103—109 (1968)

Alving, B.O.: Spontaneous activity in isolated somata of *Aplysia* pacemaker neurons. J. gen. Physiol. **45**, 29—45 (1968)

Bullock, T.H.: The origins of patterned nervous discharge. Behavior **17**, 48—59 (1961)

Dunin-Barkovskii, V.L.: Fluctuations in the level of activity in simple closed neurone chains. Biofizika **15**, 374—378 (1970)

Friesen, W.O., Poon, M., Stent, G.S.: An oscillatory neuronal circuit generating a locomotory rhythm. Proc. Nat. Acad. Sci. USA **73**, 3734—3738 (1976)

Friesen, W.O., Poon, M., Stent, G.S.: Neuronal control of swimming in the medicinal leech. IV. Identification of a network of oscillatory interneurons. Submitted for publication (1977)

Kling, V., Székely, G.: Simulation of rhythmic nervous activities. I. Function of networks with cyclic inhibitions. Kybernetik **5**, 89—103 (1968)

Kristan, W.B., Jr., Calabrese, R.L.: Rhythmic swimming activity in neurons of the isolated nerve cord of the leech. J. exp. Biol. **63**, 643—666 (1976)

Kristan, W.B., Jr., Stent, G.S., Ort, C.A.: Neuronal control of swimming in the medicinal leech. I. Dynamics of the swimming rhythm. J. comp. Physiol. **94**, 97—119 (1974a)

Kristan, W.B., Jr., Stent, G.S., Ort, C.A.: Neuronal control of swimming in the medicinal leech. III. Impulse patterns of the motor neurons. J. comp. Physiol. **94**, 155—176 (1974b)

Lewis, E.R.: Using electronic circuits to model simple neuroelectric interactions. Proc. Inst. Elec. Electron Engrs. **56**, 931—949 (1968)

Ort, C.A., Kristan, W.B., Jr., Stent, G.S.: Neuronal control of swimming in the medicinal leech. II. Identification and connections of motor neurons. J. comp. Physiol. **94**, 121—154 (1974)

Perkel, D.H., Mulloney, B.: Motor pattern production in reciprocally inhibitory neurons exhibiting postinhibitory rebound. Science **185**, 181—183 (1974)

Poon, M.: A neuronal network generating the swimming rhythm in the leech. Ph. D. Thesis, Univ. of California, Berkeley, Calif. 1976

Poon, M., Friesen, W.O., Stent, G.S.: Neural control of swimming in the medicinal leech. V. Connections between the oscillatory interneurons and the motor neurons. Submitted for publication (1977)

Pozin, N.V., Shulpin, Yu.A.: Analysis of the work of auto-oscillatory neurone junctions. Biofizika **15**, 156—163 (1970)

Reiss, R.F.: A theory and simulation of rhythmic behavior due to reciprocal inhibition in small nerve nets. Am. Fed. Inf. Process Soc. Proc. Spring Joint Computer Conference **21**, 171—194 (1962)

Székely, G.: Logical network for controlling limb movement in urodela. Acta Physiol. Acad. Sci. Hung. **27**, 285—289 (1965)

Wilson, D.M.: Central nervous mechanisms for the generation of rhythmic behavior in arthropods. In: Nervous and hormonal mechanisms of integration. Symp. Soc. Exp. Biol. **20**, 199—228 (1966)

Wilson, D.M., Waldron, I.: Models for the generation of the motor output pattern in flying locusts. Proc. Inst. Elec. Electron, Engrs. **56**, 1058—1064 (1968)

Received: July 26, 1977

Prof. G. S. Stent
Dept. of Molecular Biology
Univ. of California
Berkeley, CA 94720, USA